PROCEEDINGS, 43rd Workshop on Geothermal Reservoir Engineering
Stanford University, Stanford, California, February 12-14, 2018
SGP-TR-213

Seismic Source Mechanism Estimation in 3D Elastic Media

Gregory A. Newman and Peter V. Petrov

Lawrence Berkeley National Laboratory, Earth Sciences Division, CA, USA

Corresponding author: gnewman@lbl.gov

Keywords: Seismic moment tensor; reciprocity, 3-D inversion; Raft River Geothermal Field, SIGMA-V

ABSTRACT

We recently developed a novel method based upon reciprocity principles to estimate seismic moment tensor estimation of localized induced and natural seismicity arising in 3D heterogeneous media. The method finds the optimal event location and corresponding moment tensor estimates. Because the method uses an exhaustive search of the 3D media it is globally convergent. It does not suffer from local minima realization observed with local optimization methods, including Newton, Gauss-Newton or gradient descent algorithms. The computational efficiency of our scheme is derived from the reciprocity principle, where the number of 3D model realizations corresponds to the number of measurement detectors. 3D forward modeling is carried out in the damped Fourier domain with the 3D finite-difference code that generates P- and S-waves from the point sources defined by second-order moment tensors. We present results of testing this new FWI moment tensor methodology on the synthetic data for the Raft River geothermal field, Idaho, as well as demonstrate its applicability in designing optimal borehole monitoring arrays in the SIGMA-V fracking experiment at the Homestake Mine, South Dakota. The SIGMA-V experiment seeks to better understand the relationship between stress, seismicity and permeability enhancement in order to advance enhance geothermal system development.

1. INTRODUCTION

During the last years the considerable attention have been turned for monitoring microseismic events in hydraulic fracturing as a diagnostic tool for fracture growth. Another problem demands increasing attention concerned with induced seismicity not only because it potentially has damaging effects, but also can be used to characterize reservoir compaction due to oil/gas and geothermal steam production. These events are characterized by small magnitude and more high frequency than their tectonic counterparts. Frequency content of microseismic events and small magnitude induce seismicity usually ranges between 2 Hz-100 Hz, 2 to 3 orders higher in frequency than the tectonic ones (Li et al., 2011). Analysis of such events is more challenging because of complicated wavefields. For example, in reservoirs with faults and strong horizontal velocity variations, ray-tracing is often challenged. Even when ray-tracing succeeds, it is very likely that one particular phase is predicted while a different phase is picked in the observed data, resulting in phase mismatch and mislocation of events. Therefore, it would be desirable if waveforms can be directly utilized to locate the events and moment tensor inversion. Unfortunately, if observed waveforms are used directly, we need to generate synthetic waveforms for matching. Since the source locations unknown, we need to test synthetic traces from all possible source locations. Additionally, since our velocity model is only an approximation to the true subsurface structure, the higher the frequencies we want to use and the larger the source-receiver distance, the greater the probability of cycle skipping between observed and predicted waveforms resulting in a local minima realization in the inversion process.

In this paper we present a novel full waveform method based on the reciprocity theorem that addresses the aforementioned challenges to efficiently locate events while performing simultaneous full moment tensor inversion of the events.

2. METHODOLOGY

The methodology of joint location and moment inversion requires a 3D velocity model of subsurface volume for potential locations and source moment of the events. It seeks to match of observed waveform data in Laplace-Fourier domain. The 3D velocity model is a priori information, which may be obtained from previous studies and derived from well cores, active source data or sonic logs. We propose that detectors record displacement velocity components $\mathbf{v}\left(\mathbf{x}_q,t\right)$ of the wave generated by a seismic event.

$$\mathbf{d}_q^{obs}\left(t\right)=\int_0^\infty \mathbf{G}\left(t-t'\right)\mathbf{v}\left(\mathbf{x}_q,t'\right)dt',\ \ q=1...N_q\ , \tag{1}$$

where $\mathbf{G}\left(t\right)$ is an the instrument response of the recorded seismogram.

The observed time–domain waveforms $\mathbf{d}_q^{obs}\left(t\right)$ are transformed to Laplace-Fourier domain for the set of different complex frequencies $s_j=\sigma_j+i\omega_j$ ($i=\sqrt{-1}$):

$$\mathbf{d}_q^{obs}\left(s_j\right)=G\left(s_j\right)\mathbf{v}_q\left(s_j\right);\mathbf{v}_q\left(s_j\right)=\int_0^\infty \mathbf{v}\left(\mathbf{x}_q,t\right)e^{-s_j t}dt,\ \ j=1...N_s,\ q=1...N_q. \tag{2}$$

where σ_j is the Laplace damping constant; ω_j is the angular frequency. Below for the simplicity we propose $G\left(s_j\right)=1$

The wavefield $\mathbf{v}\left(\mathbf{x}_q,s_j\right)$ is the solution at point $\mathbf{x}_q$ of the elastic equations in the Laplace-Fourier domain, which can be directly obtained taking the integral transform of the time-domain system for velocity and stress formulation (Virieux, 1986)

$$\begin{aligned}
&s_j\rho\mathbf{v}=\mathbf{D}_\tau\boldsymbol{\tau}+\mathbf{f}\left(\mathbf{x},s_j\right),\\
&s_j\boldsymbol{\tau}=\mathbf{D}_v\left(\kappa,\mu\right)\mathbf{v}+s_j\mathbf{m}\left(\mathbf{x},s_j\right),\\
&\mathbf{v}=\left(v_x,v_y,v_z\right)^T,\boldsymbol{\tau}=\left(\tau_{xx},\tau_{xy},\tau_{xz},\tau_{yy},\tau_{yz},\tau_{zz}\right)^T,\\
&\mathbf{m}=\left(m_{xx},m_{xy},m_{xz},m_{yy},m_{yz},m_{zz}\right)^T
\end{aligned} \tag{3}$$

where v_x,v_y,v_z are the velocity wave-field components, $\tau_{pq};p,q\in\left(x,y,z\right)$ are the stress tensor components, $\mathbf{f}$ is body force per unit volume, $\mathbf{m}$ is the moment tensor density of a seismic event, symbols $\mathbf{D}_\tau,\mathbf{D}_v\left(\kappa,\mu\right)$ respectively denote the partial differential operators, where $\kappa\left(\vec{r}\right)$ and $\mu\left(\vec{r}\right)$ are elastic bulk and share moduli of the media (Petrov, Newman 2012, 2014).

The general reciprocity theorem for the elastic equations (3) gives the next integral expression, which connects parameters of a seismic source m_{ij},f_i and velocity component $v_i\left(\mathbf{x}\right)$ at position $\mathbf{x}$ (Aki and Richards, 2009; Aldridge and Symons, 2001):

$$\int dV\left(m_{ij}\partial_j v_i^R+f_i v_i^R-f_l^R\left(\mathbf{x}\right)v_l\left(\mathbf{x}\right)\right)=0\,,\ i,j,l=x,y,z \tag{4}$$

Here $f_l^R\left(\mathbf{x}\right)$ is some force applied in the same direction l and position $\mathbf{x}$ as velocity $v_l\left(\mathbf{x}\right)$, v_i^R is the velocity component generated by this force. It should be noted that both velocities $\mathbf{v},\mathbf{v}^R$ satisfy the same system of equation (3) but with different source terms.

Since usually a receiver measures velocity at a fix point $\mathbf{x}_q$ let's define forces $f_l^R\left(\mathbf{x}\right)$ other than zero only at the receiver position $\mathbf{x}_q$ for each $q=1...N_q$:

$$f_l^R\left(\mathbf{x}\right)=f_l^q\delta\left(\mathbf{x}-\mathbf{x}_q\right). \tag{5}$$

In this case, relation (4) can be rewritten as follows

$$\int\left(m_{ij}\left(\mathbf{x}\right)\partial_j v_i^R\left(\mathbf{x}\right)+f_i\left(\mathbf{x}\right)v_i^R\left(\mathbf{x}\right)\right)dV=f_l^R\left(\mathbf{x}_q\right)v_l\left(\mathbf{x}_q\right),\ i,j,l=x,y,z\,;q=1...N_q \tag{6}$$

The point source is defined by the moment tensor $\mathbf{M}^S$ at position $\mathbf{x}_s$

$$\mathbf{m}^s\left(\mathbf{x}\right)=\mathbf{M}^s\delta\left(\mathbf{x}-\mathbf{x}_s\right)\ . \tag{7}$$

Here we assume there is no need for a body force for the point source description. The integral relationships transform to a system of linear equations

$$\sum_{i,j}M_{ij}^s\partial_j v_i^{R_q}\left(\mathbf{x}_s\right)=\sum_l f_l^{R_q}v_l\left(\mathbf{x}_q\right),\ i,j,l=x,y,z;\,q=1..N_q \tag{8}$$

For the simplicity let's assume that each receiver measures only one velocity component v_l . It means that if a receiver measures all three components of the velocity field we consider it as three independent receivers at the same space point but with different velocity components. Equation (8) results in:

$$\sum_{i,j}M_{ij}^s\partial_j v_i^{q,k}\left(\mathbf{x}_s\right)=f_k^q v_k\left(\mathbf{x}_q\right),\ i,j,k=x,y,z;\,q=1..N_q \tag{9}$$

Here $v_i^{q,k}(\mathbf{x}_s)$ is the value at $\mathbf{x}_s$ i - component of the velocity generated by k - component of force placed at receiver position $\mathbf{x}_q$.

Because (9) are valid for any values of f_k^q different from zero we set f_k^q be equal to $1/v_k(\mathbf{x}_q)$ and obtain a system, where the number of equations is equal to the number of "one component" receivers N_d

$$\begin{aligned} &M_{xx}^S \partial_x v_x^{q,k}(\mathbf{x}_s) + M_{yy}^S \partial_y v_y^{q,k}(\mathbf{x}_s) + M_{zz}^S \partial_z v_z^{q,k}(\mathbf{x}_s) + \\ &M_{xz}^S \left(\partial_z v_x^{q,k}(\mathbf{x}_s) + \partial_x v_z^{q,k}(\mathbf{x}_s)\right) + M_{xy}^S \left(\partial_y v_x^{q,k}(\mathbf{x}_s) + \partial_x v_y^{q,k}(\mathbf{x}_s)\right) + \\ &+ M_{yz}^S \left(\partial_y v_z^{q,k}(\mathbf{x}_s) + \partial_z v_y^{q,k}(\mathbf{x}_s)\right) = 1 \end{aligned} \tag{10}$$

or the matrix form

$$\begin{aligned} &\mathbf{B}\mathbf{M}^s = \mathbf{E}; \\ &\mathbf{B} = \begin{bmatrix} \partial_x v_x^1 & \partial_y v_x^1 + \partial_x v_y^1 & \partial_z v_x^1 + \partial_x v_z^1 & \partial_y v_y^1 & \partial_y v_z^1 + \partial_z v_y^1 & \partial_z v_z^1 \\ \dots & & & & & \\ \partial_x v_x^{N_d} & \partial_y v_x^{N_d} + \partial_x v_y^{N_d} & \partial_z v_x^{N_d} + \partial_x v_z^{N_d} & \partial_y v_y^{N_d} & \partial_y v_z^{N_d} + \partial_z v_y^{N_d} & \partial_z v_z^{N_d} \end{bmatrix}_{\mathbf{x}=\mathbf{x}_s}; \end{aligned} \tag{11}$$

Instead of calculating $\mathbf{B}$ at the source position, which is unknown we can define it everywhere inside a region of possible event locations. For this purpose it is necessary to obtain N_d different solutions of elastic equations for each "one component" receiver separately:

$$\begin{aligned} &s_j \rho \mathbf{v}^{q,k} = \mathbf{D}_\tau \boldsymbol{\tau} + \mathbf{f}_k(\mathbf{x}_q), \ k = x,y,z; q = 1..N_q \\ &s_j \boldsymbol{\tau} = \mathbf{D}_v(\kappa,\mu)\mathbf{v}^{q,k}, \quad \mathbf{f}_k(\mathbf{x}_q) = 1/v_k(\mathbf{x}_q)\cdot\mathbf{k} \end{aligned} \tag{12}$$

and perform differentiation on the velocity field. Here $\mathbf{k}$ is a unit vector directed along measured velocity component $v_k(\mathbf{x}_q)$.

Uniqueness of the elastic problem solution guarantees only one point $\mathbf{x}_s$, where all equations are true. For all other points $\mathbf{x} \neq \mathbf{x}_s$ the reciprocity condition will be violated. That means that the problem of the source position and moment tensor definition can be solved by searching for a point inside the region, where all equations are satisfied or effectively minimizing the objective functional Q expressed by the residuals between vectors $\mathbf{B}\mathbf{M}^s$ and $\mathbf{E}$. At the correct source position we would have

$$Q(\mathbf{B}\mathbf{M} - \mathbf{E}) = 0 \ , \tag{13}$$

but with measurement noise and unknown errors in the assumed velocity model we seek a minimum in the objective function, instead. This minimization can be easily and very efficiently realized by exhaustive search for all possible space points. For this purpose, for each $\mathbf{x}$ in the examination region the solution of normalized equation is defined:

$$\mathbf{M}(\mathbf{x}) = \left(\mathbf{B}^T(\mathbf{x})\mathbf{B}(\mathbf{x})\right)^{-1} \cdot \mathbf{B}^T(\mathbf{x})\mathbf{E} \tag{14}$$

And response at the receiver's position is calculated

$$\mathbf{q}_\mathbf{x} = \mathbf{B}(\mathbf{x})\mathbf{M}(\mathbf{x}) \tag{15}$$

Vector $\mathbf{q}_\mathbf{x} = \left(q_{\mathbf{x},1} \quad q_{\mathbf{x},2} \quad \dots \quad q_{\mathbf{x},N_d}\right)$ is taken for the construction of the objective function

$$Q(\mathbf{x}) = \left| \prod_{l=1}^{N_d} q_{\mathbf{x}l} - 1 \right| \tag{16}$$

The source position is determined by exhaustive search for point $\mathbf{x}_s^{inv}$, where Q has minimum, close to the zero

$$\min_{\mathbf{x}}\left(Q(\mathbf{x})\right)\Rightarrow 0\,. \tag{17}$$

The main advantages of such approach are concerned with the unique definition of the minimum of (17) that does not require non linear inversion iterations and provides a simultaneous definition of the moment tensor, which can be obtained by equation (14) at point $\mathbf{x}_s^{inv}$

$$\mathbf{M}_{inv}^{s}=\left(\mathbf{B}^T\left(\mathbf{x}_s^{inv}\right)\mathbf{B}\left(\mathbf{x}_s^{inv}\right)\right)^{-1}\cdot\mathbf{B}^T\left(\mathbf{x}_s^{inv}\right)\mathbf{E} \tag{18}$$

For the exact velocity model of media and data without any noise this method gives the exact position of the point seismic event and it moment tensor.

For the fix position of survey there is no necessity to solve system (12) for the inversion of each seismic event over again. It is enough to solve it once for $\mathbf{f}_k\left(\mathbf{x}_q\right)=\mathbf{k}, q=1...N_d$. As a matter of fact this is the calculation of strain Green's tensor (Zhao, Chen, and Jordan,2006). Because of linearity the elastic problem, elements of matrix $\mathbf{B}$ will be defined by multiplying corresponding rows of strain Green's tensor by factor , $1/v_k\left(\mathbf{x}_q\right)$ which are defined by current seismic event. The following definition of a source location and moment tensor (14)-(18) is fast because it does not require expensive calculation and may be very efficient for seismic monitoring applications.

If the moment tensor has some space distribution different from point source distribution, then the minimum of (17) cannot reach zero and instead of algebraic system (10) we still have N_d integral relations:

$$\begin{aligned}&\int_{V_1} m_{xx}^{S}(\mathbf{x})\partial_x v_x^{q,k}(\mathbf{x})dV+\int_{V_4} m_{yy}^{S}(\mathbf{x})\partial_y v_y^{q,k}(\mathbf{x})dV+\int_{V_6} m_{zz}^{S}(\mathbf{x})\partial_z v_z^{q,k}(\mathbf{x})dV+\\&\int_{V_3} m_{xz}^{S}(\mathbf{x})\left(\partial_z v_x^{q,k}(\mathbf{x})+\partial_x v_z^{q,k}(\mathbf{x})\right)dV+\int_{V_2} m_{xy}^{S}(\mathbf{x})\left(\partial_y v_x^{q,k}(\mathbf{x})+\partial_x v_y^{q,k}(\mathbf{x})\right)dV+\\&+\int_{V_5} m_{yz}^{S}(\mathbf{x})\left(\partial_y v_z^{q,k}(\mathbf{x})+\partial_z v_y^{q,k}(\mathbf{x})\right)dV=1\end{aligned} \tag{19}$$

where integration performs over the volumes $V_d,(d=1...5)$.

The simplifying assumption is to suppose each moment tensor component be a constant inside the defined volume and after implementation of the mean-value theorem it can be rewritten as:

$$\begin{aligned}&M_{xx}^{VS}\left\langle\partial_x v_x^{q,k}\right\rangle_{v_1 1}+M_{yy}^{VS}\left\langle\partial_y v_y^{q,k}\right\rangle_{V_4}+M_{zz}^{VS}\left\langle v_z^{q,k}\right\rangle_{V_6}+\\&M_{xz}^{VS}\left\langle\partial_z v_x^{q,k}+\partial_x v_z^{q,k}\right\rangle_{V_3}+M_{xy}^{VS}\left\langle\partial_y v_x^{q,k}+\partial_x v_y^{q,k}\right\rangle_{V_4}+M_{yz}^{VS}\left\langle\partial_y v_z^{q,k}+\partial_z v_y^{q,k}\right\rangle_{V_5}=1\\&\left\langle\partial_i v_j^{q,k}\right\rangle_{V_k}=\frac{\int_{V_k}\partial_i v_j^{q,k}(\mathbf{x})dV}{V_k};\\&M_{xx}^{VS}=m_{xx}V_1;\ M_{xy}^{VS}=m_{xy}^{S}V_2;M_{xz}^{VS}=m_{xz}^{S}V_3;M_{yy}^{VS}=m_{yy}^{S}V_4;M_{yz}^{VS}=m_{yz}^{S}V_5;M_{zz}^{VS}=m_{zz}^{S}V_6\end{aligned} \tag{20}$$

The system (20) has the same structure as equations (10) but instead of calculating velocity derivatives at a point it is necessary to calculate them over some unknown volumes. For this case the minimum of objective function Q_{distr} can be provided in two steps. First, the hypocenter and moment tensor of the seismic event are defined by (17)-(18). Second, using information about the moment tensor of a point source the different configurations of specific volumes $V_d,(d=1...5)$ can be tested through the different patterns in size and form around $\mathbf{x}_s^{inv}$ by the additional exhaustive search. The optimal configuration is realized when $Q_{distr}<Q_{point}\left(\mathbf{x}_s^{inv}\right)$.

So, the global minimum for distributed seismic source is defined by the exhaustive search for hypocenter and different patterns around it.

The described method defines event location and moment tensor for the fix complex frequency. To define the evolution of moment tensor in the time domain it is necessary to perform inversion for the set of frequencies through inverse Laplace-Fourier transformation.

3. SYNTHETIC EXAMPLES

When making reference to previous work, please follow the scientific format, e.g. Verma and Pruess (1976).

3.1 Raft River 3-D elastic model

3.1.1 Point source parameters inversion

For the algorithm validation we use the part of 3D Raft River velocity model designed by Nash and Moore (2012). To reduce both the required memory and computing time, we used a part of this model, which contains eight LBNL seismic stations. The model is rotated so that Narrows Zone aligns along the X-axis with a broadside extension of $396 \le x \le 5724, 1068 \le y \le 5148$ (in meters). The depth extend of the model is $0 \le z \le 2256$ (in meters). The distribution of P-wave velocities in the planes $x = 3600$ and $z = 2000$ m are shown in Figures 2. Synthetic data were generated by the Laplace-Fourier domain finite-difference modeling technique (Petrov and Newman 2012). The number of grid nodes was $111 \times 85 \times 47$ with the grid spacing of 48 m. A free surface boundary condition was imposed on the surface z=0. On the other boundaries the perfectly match layer (PML) boundary condition was applied.

Each seismic station records three components of velocity displacement near the surface. So, there are twenty four "one component" receivers in eq. (12) $N_d = 24$. The projections of survey geometry are presented in Figure 2. The position of microseismic source was near the Narrows zone at point $x_s = 3996, y_s = 3612, z_s = 1680$ meters. The value of the normalized moment tensor included all 6 components:

$$\mathbf{M}^s_{exc} = \begin{bmatrix} 0.5 & 0.2 & 1.0 \\ 0.2 & 0.5 & 0.1 \\ 1.0 & 0.1 & -1.0 \end{bmatrix} \tag{21}$$

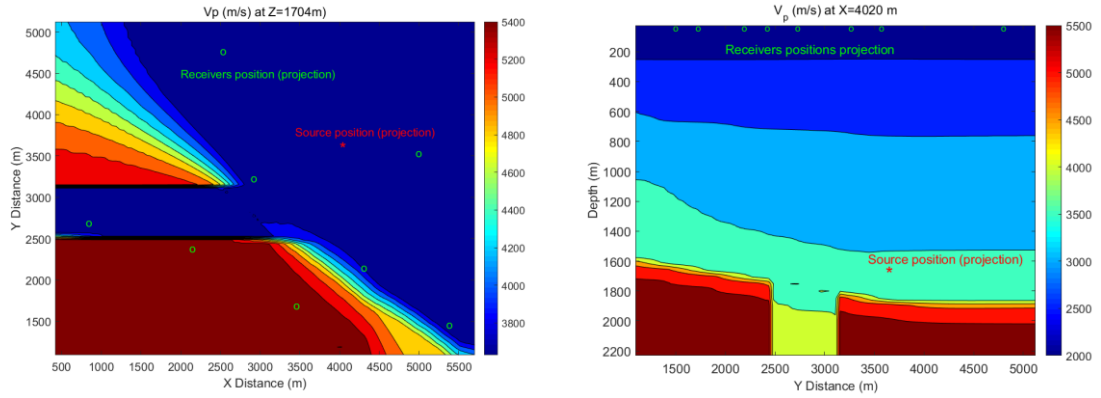

Figure 1: P-wave velocities of the Raft River elastic model and seismic survey geometry.

The inversion was performed at frequency f =3 Hz with damping constant $\sigma = 6$ 1/s. The behavior of objective function Q is shown in Figure 2.

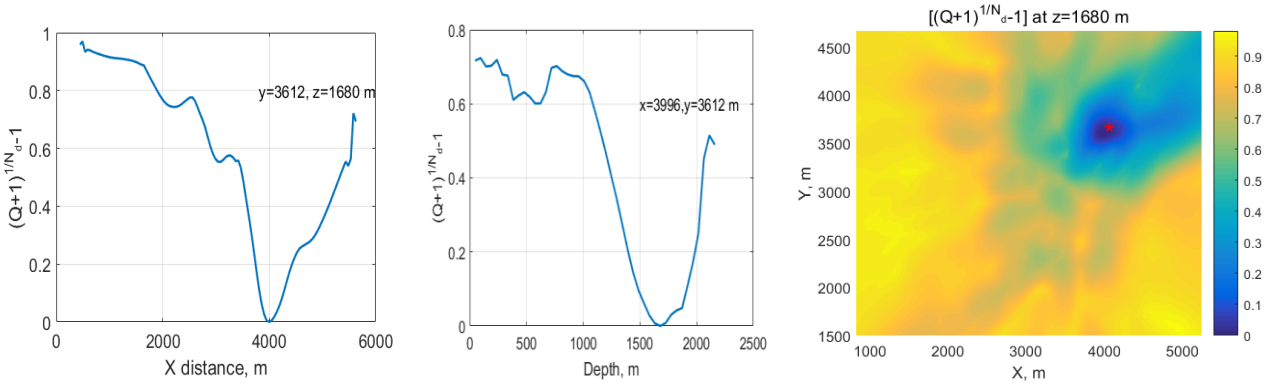

a) b) c)

Figure 2: Profile of objective function along X-distance (a), profile of objective function along depth (b), distribution of objective function in XY- plane at the source depth

The minimum of Q gives exact location and moment tensor of the point source within the accuracy of numerical solution.

$$\mathbf{M}_{inv}^{s} = \begin{bmatrix} 0.4992+10^{-4}i & 0.1998 & 1.0002+3\cdot10^{-4}i \\ 0.1998 & 0.5002++3\cdot10^{-4}i & 0.0999 \\ 1.0002+3\cdot10^{-4}i & 0.0999 & -0.9998+4\cdot10^{-4}i \end{bmatrix} \quad (22)$$

3.1.2 Stochastic data noise and velocity model uncertainty influence

For the estimation of the data noise influence on inverted results, random Gaussian noise (with the variance equal to 5 and 10%) $\Delta\mathbf{d}_q^{obs}$ was added to the synthetic data $\mathbf{d}_q^{obs}$:

$$\mathbf{d}_q^{stc} = \mathbf{d}_q^{obs} + \Delta\mathbf{d}_q^{obs},\ q = 1...N_q. \quad (23)$$

The exact velocity model was applied. Inversion with 100 realizations of different values $\Delta\mathbf{d}_q^{obs}$ shows that stochastic noise in data does not have essential influence to the source location definition. Deviation from the exact location is not more than one cell size. Moment-tensor components are more sensitive to the magnitude of the noise (Table 1) but for the largest components it keeps the same level of errors as data noise.

To investigate sensitivity inversion to the velocity model we generated three inexact models, which were obtained by smoothing the all attributes of exact distribution (density, V_s,V_p) (Petrov, Newman, 2017). The difference between models is characterized by the relative error:

$$e_m = \left\| V_{p,s}^{exact} - V_{p,s}^{smooth} \right\| \Big/ \left\| V_{p,s}^{exact} \right\| * 100\% \quad (24)$$

Despite the difference between exact and assumed models, the errors in the estimated source coordinates are less than one cell size (Table 1), but moment-tensor elements are more sensitive to the assumed velocity model. Increasing errors e_m leads to the corresponding errors in the moment tensor estimates, although relations between different components are still approximately conserved (Table 1).

.

Table 1: Influence of data stochastic errors and velocity model uncertainty for moment tensor inversion

Moment tensor components	Exact value	Inverted value for inexact model $e_m = 6\%$	Inverted value for inexact model $e_m = 9\%$	Inverted value for inexact model $e_m = 12\%$	Deviation from exact values (%) for data stochastic noise 5% and exact model	Deviation from exact values (%) for data stochastic noise 10% and exact model
M_{xx}	0.5	0.445	0.1	-0.22	7	23.7
M_{xy}	0.2	0,255	0.15	0.03	5.8	24.8
M_{xz}	1.0	0.89	0.91	0.82	2.2	8.5
M_{yy}	0.5	0.44	0.23	0.14	4.2	10.4
M_{yz}	0.1	0.0255	0.034	0.07	14.3	85.6
M_{xx}	-1	-0.864	-0.94	-0.825	3.1	7.5

3.2 SIGMA-V fracking experiment

The SIGMA-V fracking experiment is the part of the EGS Collab project (Dobson et al, 2017). This project provides the basis to better understanding of the creation of fracture geometries during stimulation, and possibilities to imaging them. This is an important problem with important applications in stimulating enhanced geothermal systems. In the SIGMA-V experiment, comprehensive micro-seismic instrumentation will be used to collect high-quality and high resolution data, along with other types of geophysical measurements for fracture characterization and fluid flow. The experiment is within a drift located approximately 1.6 km beneath the surface. Four parallel boreholes and two orthogonal boreholes are used to acquire seismic data during the experiment (Figure 3a). One of the key parameters of fracture characterization is moment tensors and location of microseismic events. We use the same borehole configuration and

geophone distribution to conduct numerical study on sensor locations and components in order to assess the accuracy of moment-tensor inversion in an experiment design study. For simplicity the Z-axis is defined along the production well (Figure 3b).

3.2.1 Source parameters inversion

We propose eleven receiver positions in each monitoring well with a 3 meter interval. According to the experiment scheme the fracture zones will be in three planes perpendicular to the production well at z=-12, 0 and 12 meters. For each plane 16 different seismic source positions were examined at $x_s, y_s = (\pm4,\pm4),(\pm8,\pm8),(\pm12,\pm12),(\pm16,\pm16)$ meters. In each case moment tensor components were $M_{xx} = 0.1; M_{xy} = 0.06; M_{xz} = 0.04; M_{yy} = 0.1; M_{yz} = 0.04; M_{zz} = -1$. We assumed the surrounding media homogeneous with $V_p = 5500, V_s = 2300$ m/s and density 2300 kg/m^3. Synthetic data were generated by the Laplace-Fourier domain finite-difference modeling technique (Petrov and Newman 2012) with cell size 0.5 m. The inversion was performed for frequencies 100 and 300 Hz with damping constant 6 s^{-1}. The typical result of the source location inversion is shown in Figure 4 for the source position $x_s = -8, y_s = -8, z_s = 0$ m and 36 one-component receivers directed along wells (6 receivers with interval 6m in each well). The inverted moment tensor coincidences with the exact one.

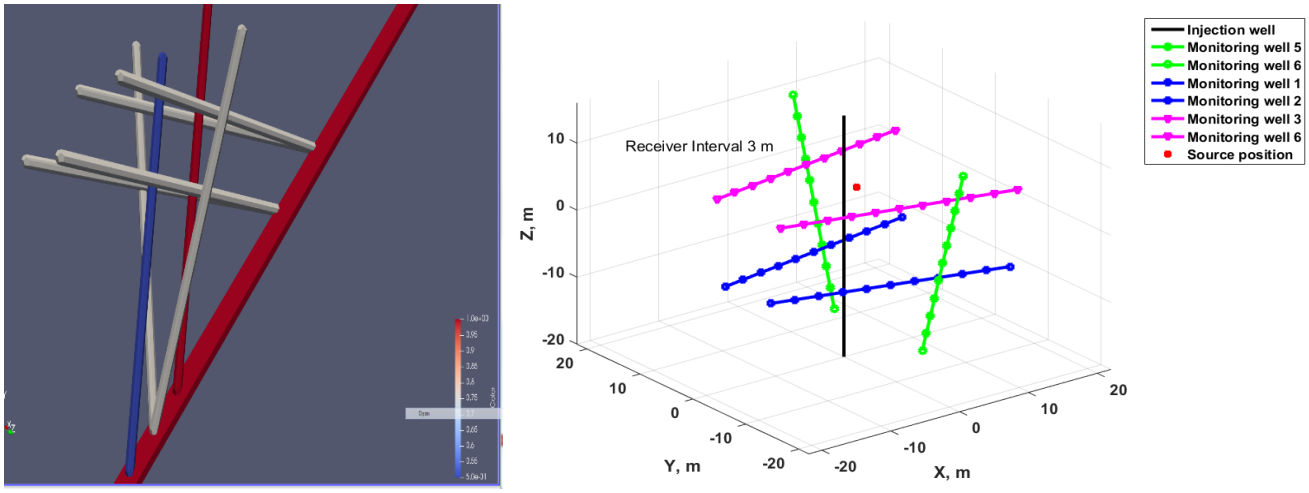

a) b)

Figure 3: Experiment geometry (blue is injection well, red -production wells, gray-monitoring wells (a). simulation geometry (b)

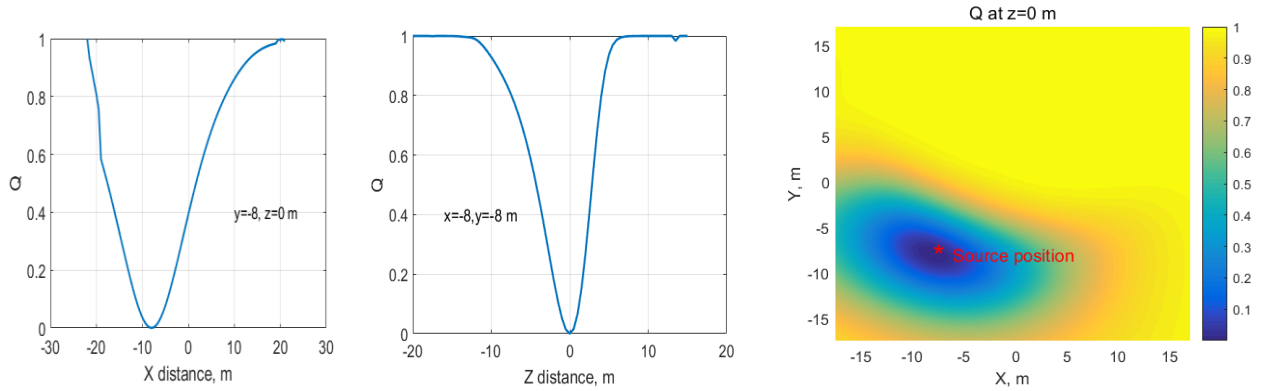

a) b) c)

Figure 4: Profile of objective function along X-distance (a), profile of objective function along depth (b), distribution of objective function in XY- plane at the source depth

We considered more than 60 different configurations of survey in three and four wells:

- one-component receivers along well direction;
- one-component receivers perpendicular to the well direction;
- three-component receivers;
- combination of one-component receivers with different directions in different wells;
- combination of one- and three-component receivers in different wells.

For all source positions and all variants of survey our method gave correct position of seismic event and exact value of moment tensor.

However the sensitivity of different surveys to the data noise are different and may be estimated from properties of $\left(\mathbf{B}^T\left(\mathbf{x}_s^{inv}\right)\mathbf{B}\left(\mathbf{x}_s^{inv}\right)\right)^{-1}$:

$$\delta\mathbf{M} \sim \left\|\left(\mathbf{B}^T\left(\mathbf{x}_s^{inv}\right)\mathbf{B}\left(\mathbf{x}_s^{inv}\right)\right)^{-1}\right\|\delta\mathbf{d}^{obs} \approx \frac{\lambda_{\max}}{\lambda_{\min}}\delta\mathbf{d}^{obs} \tag{25}$$

where condition number= $\frac{\lambda_{\max}}{\lambda_{\min}}$ is the relation of largest eigenvalue of matrix $\left(\mathbf{B}^T\left(\mathbf{x}_s^{inv}\right)\mathbf{B}\left(\mathbf{x}_s^{inv}\right)\right)^{-1}$ to the smallest one

The small condition numbers correspond to robust configurations. For current design of monitoring wells (Figure 3) the most robust and worse configurations for one component receivers are shown in Table 2:

Table 2: Robustness of one-component receivers survey

Configuration						Condition number
Direction in Well #1	Direction in Well #2	Direction in Well #3	Direction in Well #4	Direction in Well #5	Direction in Well #6	Max condition number
z	z	z	x	x	x	26
z	z	z	z	x	x	26.7
z	x	z	z	x	z	25.7
y	z	z	y	x	x	26.2
z	y	x	x	x	x	115

For the three-component receivers the configuration close to optimal is 3 receivers with interval 15 m

3.2.2 Stochastic data noise

For the estimation of the data noise influence for inverted results random Gaussian noise (with the variance equal to 5 and 10%) was added to the synthetic data $\mathbf{d}_q^{obs}$. We examined the event situated at the boundary of investigated region $x_s = 12, y_s = 12, z_s = 0$ m and survey from one component receivers (first row in Table 2). As for the previous case (Raft River model) the influence of data stochastic noise to source location is pretty small (deviation from exact position is less than one cell size). For moment tensor the results are in Table 3. The level of error in inverted parameters corresponds to the noise level.

Table 3: Influence of data stochastic errors for moment tensor inversion

Moment Tensor component	Exact value	Gauss noise 5 %	Gauss noise 10 %
M_{xx}	0.1	15%	30%
M_{xy}	0.06	12%	20%
M_{xz}	0.04	45%	45%
M_{yy}	0.1	15%	28%
M_{yz}	0.04	5%	10%
M_{xx}	-1.0	4%	6%

6. DISCUSSION

Comparing reciprocity FWI results with the other inversion of the moment tensor is beneficial in investigating seismic events in complex 3D heterogeneous media, because it provides exact solution of the problem for the correct 3D velocity model, which may be critical for understanding physical processes if the structure of microseismic sources is considered as a marker of fluid-related processes when stimulating geothermal systems. The method is very economic because does not require any iteration process, which is characteristic of other non-linear full waveform inversion methods for source moment characterization. Moreover, with a stationary monitoring survey it is necessary to solve 3d elastic problem only N_d times, which is defined by the receivers number. As the result of this approach we obtained Laplace-Fourier image of moment tensor and theoretically after inverse transformation possibilities to define dynamic moment tensor.

The method does not request any initial approximation of a source location. The inverted source position may be different for different frequencies that theoretically allow proposing a possibility of tracking the changes in the source mechanism and position during a microearthquake in time and estimating its volume.

7. CONCLUSION

We presented a novel FWI method based on the reciprocity theorem for the estimation of microseismic sources parameters (location and moment tensor) in Laplace-Fourier domain for 3D elastic heterogeneous media. The stability of the algorithm was tested for the input data contaminated with Gaussian noise and inexact velocity models. In noise-free tests the method guarantees the exact values of the source parameters. In the variance of the noise and inexact velocity model the inversion method produces good source location and approximate values of moment tensor components with the errors corresponding to the noise magnitude and velocity model deviations. The methodology was tested on a synthetic data set generated for Raft River geothermal area and SIGMA-V experiment.

8. ACKNOWLEDGEMENT

This material was based upon work supported by the U.S. Department of Energy, Office of Energy Efficiency and Renewable Energy (EERE), Office of Technology Development, Geothermal Technologies Program, under Award Number DE-AC02-05CH11231. The United States Government retains, and the publisher, by accepting the article for publication, acknowledges that the United States Government retains a non-exclusive, paid-up, irrevocable, world-wide license to publish or reproduce the published form of this manuscript, or allow others to do so, for United States Government purposes.

9. REFERENCES

Aki, K., and P. G. Richards, 2002, Quantitative seismology:University Science Books.

Aldridge D. and Symons N., P., 2001, Seismic reciprocity rules. SEG Technical Program Expanded Abstracts 2001: pp. 2049-2052

Li, J., H. S. Kuleli, H. Zhang, and M. N. Toksöz, 2011, Focal mechanism determination of induced microearthquakes in an oil field using full waveforms from shallow and deep seismic networyb;tks: Geophysics, 76, no. 6, WC87–WC101

Dobson et al., 2017, An Introduction to the EGS Collab Project, GRC Transactions, Vol. 41, 837-849

Nash, G. D., and Moore, J. N., 2012, “Raft River EGS Project: A GIS-Centric Review of Geology”, GRC Transactions, 36, 951 - 958.

Petrov, P.V., Newman, G. A., 2012. 3D finite-difference modeling of elastic wave propagation in the Laplace-Fourier domain, Geophysics, 77, T137-T155.

Petrov P.V., Newman G. A., 2014. Three-dimensional inverse modelling of damped elastic wave propagation in the Fourier domain. Geophysical Journal International 198, 1599–1617

Petrov P.V., Newman G. A., 2017. Source moment estimation in three dimensional full waveform inversion. proceedings, 42rd Workshop on Geothermal Reservoir Engineering Stanford University, Stanford, California, February 13-15

Zhao, L., Chen, P. and Jordan, T. H., 2006, Strain Green tensor, reciprocity, and their applications to seismic source and structure studies, Bull. Seism. Soc. Am., 96, 1753-1763

Virieux, J., 1986, P-SV wave propagation in heterogeneous media: Velocity-stress finite-difference method, Geophysics **51**, 889–901.